

# TextRay: Contour-based Geometric Modeling for Arbitrary-shaped Scene Text Detection

Fangfang Wang

College of Computer Science, Zhejiang University  
fangfangliana@zju.edu.cn

Fei Wu

College of Computer Science, Zhejiang University  
wufei@zju.edu.cn

Yifeng Chen

College of Computer Science, Zhejiang University  
yifengchen@zju.edu.cn

Xi Li\*

College of Computer Science, Zhejiang University  
xilizju@zju.edu.cn

## ABSTRACT

Arbitrary-shaped text detection is a challenging task due to the complex geometric layouts of texts such as large aspect ratios, various scales, random rotations and curve shapes. Most state-of-the-art methods solve this problem from bottom-up perspectives, seeking to model a text instance of complex geometric layouts with simple local units (e.g., local boxes or pixels) and generate detections with heuristic post-processings. In this work, we propose an arbitrary-shaped text detection method, namely TextRay, which conducts top-down contour-based geometric modeling and geometric parameter learning within a single-shot anchor-free framework. The geometric modeling is carried out under polar system with a bidirectional mapping scheme between shape space and parameter space, encoding complex geometric layouts into unified representations. For effective learning of the representations, we design a central-weighted training strategy and a content loss which builds propagation paths between geometric encodings and visual content. TextRay outputs simple polygon detections at one pass with only one NMS post-processing. Experiments on several benchmark datasets demonstrate the effectiveness of the proposed approach. The code is available at <https://github.com/LianaWang/TextRay>.

## CCS CONCEPTS

• **Computing methodologies** → **Object detection; Supervised learning by regression; Neural networks.**

## KEYWORDS

Arbitrary-shaped Text Detection, Geometric Modeling

## ACM Reference Format:

Fangfang Wang, Yifeng Chen, Fei Wu, and Xi Li. 2020. TextRay: Contour-based Geometric Modeling for Arbitrary-shaped Scene Text Detection. In *Proceedings of the 28th ACM International Conference on Multimedia (MM '20, October 12–16, 2020, Seattle, WA, USA)*

\*Corresponding author.

Permission to make digital or hard copies of all or part of this work for personal or classroom use is granted without fee provided that copies are not made or distributed for profit or commercial advantage and that copies bear this notice and the full citation on the first page. Copyrights for components of this work owned by others than ACM must be honored. Abstracting with credit is permitted. To copy otherwise, or republish, to post on servers or to redistribute to lists, requires prior specific permission and/or a fee. Request permissions from [permissions@acm.org](mailto:permissions@acm.org).

MM '20, October 12–16, 2020, Seattle, WA, USA  
© 2020 Association for Computing Machinery.  
ACM ISBN 978-1-4503-7988-5/20/10...\$15.00  
<https://doi.org/10.1145/3394171.3413819>



**Figure 1: Demonstration of different global representations.** (a) shows the global representation under Cartesian system: the three instances are represented with variable-length points (e.g., 6, 8 and 4 orange dots) with very subjective distribution. (b) shows the global representation under polar system: all instances are represented by a set of radiuses of same number and angular distribution (green rays).

'20), October 12–16, 2020, Seattle, WA, USA. ACM, New York, NY, USA, 9 pages.  
<https://doi.org/10.1145/3394171.3413819>

## 1 INTRODUCTION

In recent years, scene text detection has attracted a surge of research interest in computer vision community for its wide-range applications such as autonomous driving, blind navigation and scene parsing. The task of scene text detection aims to localize text areas in natural images. Despite the significant achievements in object detection, accurately detecting scene texts remains challenging due to their unique traits in geometric layouts: large aspect ratios, various scales, random rotations, and curve shapes.

Different from generic object detection which requires bounding-box outputs, scene text detection demands explicit contours of text instances. With this motivation, a lot of efforts have been paid in seeking effective contour modeling for arbitrary-shaped text representation. A typical way adopted in state-of-the-art methods is to model text instances from local perspectives. These local modeling methods usually decompose a text instance with complex geometric layout into simple control units. For example, [8, 20] represent text instances with sequential discs and local boxes, respectively. Segmentation-based methods [30, 31], which model arbitrary-shaped text instances at pixel level and represent the contours with the edge of masks, can be seen as an extreme case of local modeling method.

However, flexible as local modeling methods are, they tend to be less resistant to noises and dependant on heuristic post-processings in contour generation due to the homogenous texture within text

regions. More importantly, they commonly pay less attention to the global geometric distribution which reflects the integrated layouts of the contours. In current benchmarks, the global layouts of arbitrary-shaped text contours are represented with adaptive or fixed number of vertices under Cartesian system, as shown in Figure 1(a). But the vertices are usually not uniformly distributed and independent to each other, neglecting the constraints of global geometric layout. Besides, the nonunified representations of adaptive number of vertices are unsuitable for parameter learning within unified convolutional neural networks(CNNs). Based on these observations, we find out that a proper global modeling method which encodes contour-level geometric information into standardized representations is needed to enable unified parameter learning.

So in this paper, we propose an arbitrary-shaped scene text detection method, namely TextRay, which conducts contour-based global geometric modeling and end-to-end parameter learning within a unified framework. Inspired by recent instance segmentation work ESE-Seg [35], we model the contours under polar system. As illustrated in Figure 1(b), a polar system is constructed at each text center, then by emitting fixed number of rays from the text centers according to the same angular distribution and intersecting the contours, we obtain unified representations for different instances in the form of sets of radiuses. This unified representation can be directly regressed with common CNNs, but it does not fully exploit the intrinsic geometric patterns, for example long patterns and symmetry properties. To dig up into the geometric patterns lying in the distribution of radiuses, we abstract a higher level geometric encoding by fitting the function curve of radiuses with respect to angles. In this way, the arbitrary-shaped contours are mapped from complex shape space to unified parameter space, and the unified fitting parameters (i.e., geometric encodings) intrinsically encodes the geometric pattern information. In this work, we represent arbitrary text contours with unified geometric encodings. To make the abstract geometric encodings more learnable, we propose a bidirectionally differentiable mapping scheme between shape space and parameter space to measure the distance of geometric encodings according to visual content.

In principle, the TextRay is a single-shot, anchor-free, and fully-convolutional framework that performs joint optimization between text/non-text classification and geometric encodings regression. It adopts an end-to-end central-weighted training strategy to effectively deal with long instances which are prevalent in scene texts. TextRay densely predicts geometric encodings and outputs simple polygon detections at one pass with only one NMS post-processing step. The main contributions of this paper are as follows:

- we convert the complex text contour discovery problem into a simple parameter learning problem through global geometric modeling and propose a bidirectionally differentiable mapping scheme between shape space and parameter space for effective geometric parameter learning;
- we present a single-shot anchor-free framework with central-weighted training strategy for solving the arbitrary-shaped scene texts detection problem;
- as a light-weighted one-stage regression-based detector, the TextRay outperforms many segmentation-based or multi-stage detectors and achieves competitive results.

## 2 RELATED WORK

Over the past few years, the mainstream of scene text detection approaches has altered from traditional methods to deep learning methods. Many CNN-based methods are inspired by general object detection and segmentation frameworks like Faster-rcnn [25], SSD [14], Mask-rcnn [10] and FCN [19]. These methods can mainly be divided into two groups according to their modeling perspectives for text instances: bottom-up local modeling methods and top-down global modeling methods.

**Local modeling methods.** Local modeling methods usually decompose scene text instances into pixels or fragments. For example, segmentation-based methods [21, 38, 40] usually explore text region at pixel-level. Segmenting text instances without cluttering or missing of parts is not easy because scene texts often appear in parallel and the texture of texts is highly homogeneous. To tackle this problem, affinity information [1, 6, 17, 36] or multi-level segmentation [20, 30, 31] are utilized to guide text saliency map generation. Another typical local modeling method is the combined method that borrows techniques from both segmentation and regression methodology. Most of these methods seek pixel-level information discovery and supportive cues from object knowledge. [22] combines region segmentation with corner detection. [8, 29, 39] segment text centerlines to coarsely locate text instances and regress border offsets and local boxes to determine accurate boundaries. Most recently, [33] proposes to model the local texture information in orthogonal directions on text proposals and generate the contours by re-scoring two responses.

**Global modeling methods.** Compared with local modeling methods, global modeling methods directly model scene text instances that possess complex geometric layouts. These methods take the regression-based methodology and treat texts as a special type of object, and regress text representations within detection frameworks. [32] proposes a two-stage detector which extracts text proposals and then sequentially predicts variable-length coordinates with LSTM. [15] introduces a concise parametric representation of curved scene text using Bezier curves. [28] encodes global geometric information into affine transformations and extracts geometry-aware features by manipulating the receptive fields. [12] introduces rotation-invariant features by rotating convolutional filters for quadrilateral vertex offset regression. [7] applies discrete geometry normalization on feature maps to enhance the perception of global geometric distribution.

**Discussion.** Most local modeling methods are rather flexible and can deal with both quadrilateral and curve text detection. But this convenience is at the cost of intensive computation and multi-stage processing. Though regression-based methods achieve high performances on quadrilateral text detection, many of them are unscalable to curve text detection. So in this paper, we realize a regression-based global modeling method, namely TextRay, for arbitrary-shaped text detection. In fact, effective contour modeling for irregular objects is also an important research point in general object segmentation tasks [34, 35, 37]. Inspired by [35], we model the text contours under polar system with a set of polar radiuses and encode geometric information by fitting the distribution of radiuses with Chebyshev polynomial approximation. Instead of directly regressing the fitting coefficients in parameter space [35],

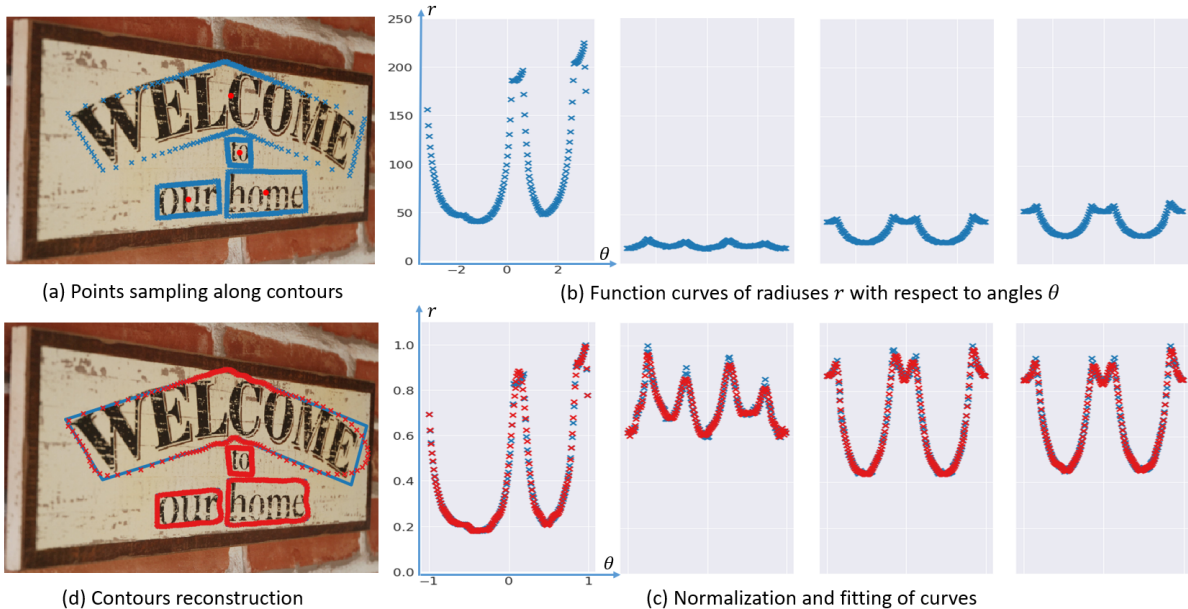


**Figure 2: Illustration of the geometric modeling for arbitrary shapes.** (a)-(c) shows the geometric encoding process and (d) shows the decoding process. In (a), points (blue crosses) are sampled along text contours by intersecting with  $N$  rays emitted from text centers (red dots); (b) visualizes the function curves (blue crosses) of radiuses  $r$  with respect to angles  $\theta$ ; in (c) the function curves are normalized (blue crosses) and fitted (red crosses) with  $K$ -degree Chebyshev polynomials; (d) displays the ground-truth contours (blue polygon) and the reconstructed contours (red crosses) from the geometric encodings.

we design a visual content-aware measurement with bidirectionally differentiable space mapping scheme to enable stable high-degree coefficients learning. Similar to the detection framework [27], our TextRay is a single-shot anchor-free framework which adopts the FPN [13] and carry out multi-level detection. Different from [27] which predicts object centerness for false positive suppression, we adopt a central-weighted training strategy to reduce the negative influence of long-shot samples during training stage.

### 3 PROPOSED METHOD

The major challenge facing arbitrary-shaped scene text detection is the complex geometric distribution of text instances. In this work, we propose a contour-based geometric modeling method that parameterizes arbitrary-shaped text contours into unified representations (i.e., geometric encodings), and effectively learn the representations within a single-shot anchor-free framework, namely TextRay.

#### 3.1 Geometric Modeling for Arbitrary Shapes

Texts in natural scenes often appear in arbitrary shapes. Instead of adopting the intuitive representation with independent vertices in Cartesian coordinates, we explore a unified representation that can reflect the intrinsic constrains of their geometric patterns. Inspired by recent work [35], we seek to represent arbitrary shapes of texts under polar system with unified geometric encodings.

Specifically, individual polar systems are constructed for different text instances. The pole of the polar system is located at the text center, which is defined as the midpoint of the text centerline. Points are sampled by intersecting the contour with  $N$  rays evenly

emitted from the text center at angles  $\theta = [\theta_1, \theta_2, \dots, \theta_N]$  from  $-\pi$  to  $\pi$  with same interval  $\Delta\theta = \frac{2\pi}{N}$  ( $N = 360$  in this case), as shown in Figure 2(a). The radiuses  $\mathbf{r} = [r_1, r_2, \dots, r_N]$  are defined as the distances between the sampled points and the text center. Note that when there are multiple intersected points, we keep the farthest one to ensure the integrity of the contour. The polar coordinates of the sampled points  $\{(\theta_i, r_i)\}_{i=1}^N$  forms a function of radiuses  $\mathbf{r}$  with respect to angles  $\theta$ , as shown in Figure 2(b). When the angular distribution is fixed, the arbitrary shapes can be represented by  $\mathbf{r}$ . However, elements in  $\mathbf{r}$  are independent and this direct representation neglects the underlying geometric patterns. To dig up into the geometric patterns and intrinsic correlations of radiuses, we map the contour from shape space to parameter space by using the Chebyshev approximation to fit the function curve. The fitting function is defined as:

$$f_K(\theta, \mathbf{c}) = \sum_{k=0}^K c_k * T_k\left(\frac{\theta}{\pi}\right), \quad (1)$$

where  $T_k$  are the Chebyshev polynomials of the first kind defined by the recurrence relation  $T_0(x) = 1, T_1(x) = x, T_k(x) = 2xT_{k-1}(x) - T_{k-2}(x)$ ,  $\pi$  is the normalization factor, and the  $K$ -degree fitting coefficients  $\mathbf{c} = [c_0, c_1, \dots, c_K]$  is defined as the *shape vector* of the instance. Instead of fitting the original  $\mathbf{r}$  of random scales, we choose to fit the normalized radiuses  $\frac{r}{s}$  ( $s = \max(\mathbf{r})$  is the scale factor for normalization) for balanced coefficients of instances in different scales. Thus  $\mathbf{c}$  is solved by the least-squares method:

$$\mathbf{c} = \underset{\mathbf{c}'}{\operatorname{argmin}} \sum_{i=1}^N \left( f_K(\theta_i, \mathbf{c}') - \frac{r_i}{s} \right)^2. \quad (2)$$

The fitted function curve is shown in Figure 2(c). Note that this fitting process is with error, which decreases with higher fitting degree  $K$ .

In this work, we define the scale of an arbitrary-shaped text as the longest sampled radius  $s$ . Together with the position  $(x, y)$ , which are the Cartesian coordinates of the text center, we obtain the unified *geometric encoding*  $\mathbf{ge} = [c, s, x, y]$  for the current instance.

Given a unique geometric encoding, we can map it from parameter space back to shape space by reconstructing the contour  $\{(x'_i, y'_i)\}_{i=1}^N$  with simple calculations:

$$\begin{aligned} r'_i &= s * f_K(\theta_i, \mathbf{c}), \\ x'_i &= x + r'_i * \cos(\theta_i), \\ y'_i &= y + r'_i * \sin(\theta_i). \end{aligned} \quad (3)$$

The reconstruction of the contour is depicted in Figure 2(d). The whole encoding and decoding process forms the global geometric modeling for arbitrary-shaped text contours.

### 3.2 Content Loss for Shape Vector Regression

Shape vector  $\mathbf{c}$  are parameters that encode the pattern of the arbitrary shape. Among the geometric properties in the geometric encoding  $\mathbf{ge} = [c, s, x, y]$ , scale  $s$  and position  $(x, y)$  are both directly related to the visual content, while  $\mathbf{c}$  is an abstracted algebraic expression of shape pattern. Directly regressing the shape vector in parameter space will neglect the intra-parameter correlations and fail to make full use of the abundant visual content. To effectively regress the shape vector, we adopt a differentiable bidirectional mapping scheme with respect to  $\mathbf{c}$  between parameter space and shape space, and incorporate the mapping into a content loss.

As illustrated in Figure 3, with the predicted shape vector  $\mathbf{c}$  and ground truth shape vector  $\mathbf{c}^*$ , we reconstruct two normalized contours whose  $i$ -th radius are  $r_i = f_K(\theta_i, \mathbf{c})$  and  $r_i^* = f_K(\theta_i, \mathbf{c}^*)$ , respectively. Scale and position are not considered in this process, so the maximum radiuses and text centers for the two contours are both 1 and the pole, respectively. The contours are in the form of  $N$  radiuses ( $N = 360$  in this case). We measure the distance between shape vectors in the parameter space by means of evaluating the differences between two sets of radiuses in the shape space:

$$L_{content}(\mathbf{c}, \mathbf{c}^*) = \frac{1}{N} \sum_i^N \text{smooth}_{L_1}(f_K(\theta_i, \mathbf{c}) - f_K(\theta_i, \mathbf{c}^*)), \quad (4)$$

where  $\text{smooth-}L_1$  function [9] is used for regression.

The differentiable content loss builds propagation paths between each radius and each parameter in the shape vector  $\mathbf{c}$ . And thus it is able to effectively model the correlations between the parameterized shape patterns and visual content.

### 3.3 Framework of TextRay

As illustrated in Sections 3.1 and 3.2, our global geometric modeling method generates learnable geometric encodings for arbitrary-shaped text instances. We embed this global geometric modeling into our TextRay framework for parameter learning.

The TextRay is a one-stage fully-convolutional framework that takes an image  $I$  as input and output simple polygon detections  $D$ . This concise framework mainly contains three parts: 1) feature

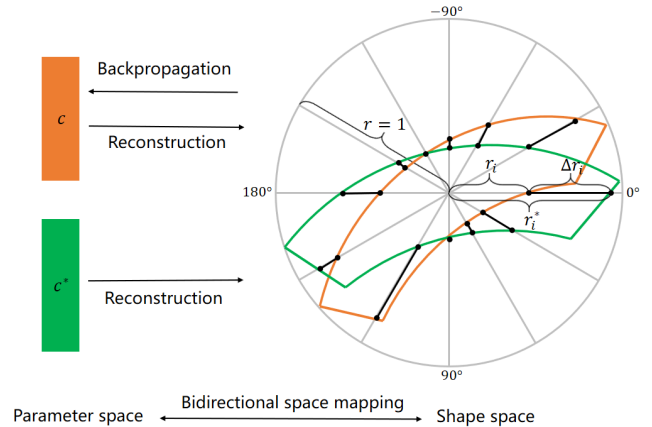


**Figure 3: Illustration of the content loss. The orange contour and the green contour are reconstructed from  $\mathbf{c}$  and the ground-truth  $\mathbf{c}^*$  respectively. The distance between the two shape vectors  $\mathbf{c}$  and  $\mathbf{c}^*$  in the parameter space is defined as the average difference between two sets of radiuses in the shape space, that is average length of the black line segments. We only display 12 radiuses for clarity.**

extraction; 2) global feature fusion; and 3) two-branch joint optimization on multi-level heads. The architecture of TextRay is depicted in Figure 4.

We utilize ResNet50 [11] as our backbone network and adopt FPN [13] to generate multi-level feature maps. P3, P4 and P5 are derived from C3, C4 and C5 of ResNet50, while P6 is generated by adding a stride two sub-sampling on top of P5.

To ensure sufficient receptive field for long instances, we adopt the SCNN\_DULR (simplified as DULR) module proposed in [23] to generate global features. In the DULR module, spatial features are propagated in four directions: bottom to top, left to right and their reverse. Particularly, we replace standard convolution along channel dimension by depth-wise convolution in DULR module to reduce network parameters. Each used pyramid top is followed by a DULR module and another  $3 \times 3$  convolutional layer.

To tackle the various scales of text instances, we predict targets of different scales at different feature levels similar to FCOS [27]. The distribution process is on the basis of relative sizes of each text instances with respect to the longer side of the input image. Different from FCOS [27], we adopt overlapping size ranges for different level, which means an instance can be simultaneously distributed to more than one level during training. The overlapping ranges is designed to maintain a higher recall rate.

On top of the feature maps, TextRay incorporates a classification branch and a regression branch. The classification branch predicts the probability of the current location being text area. And the regression branch regresses the geometric encodings (i.e., shape, scale and position) of the associated text instance. The final output  $D$  is generated by fast decoding according to Equation 3 and a Soft-NMS [2] step.

### 3.4 Central-weighted Training

To effectively learn the unified geometric encodings and optimize the anchor-free TextRay framework, we design a central-weighted



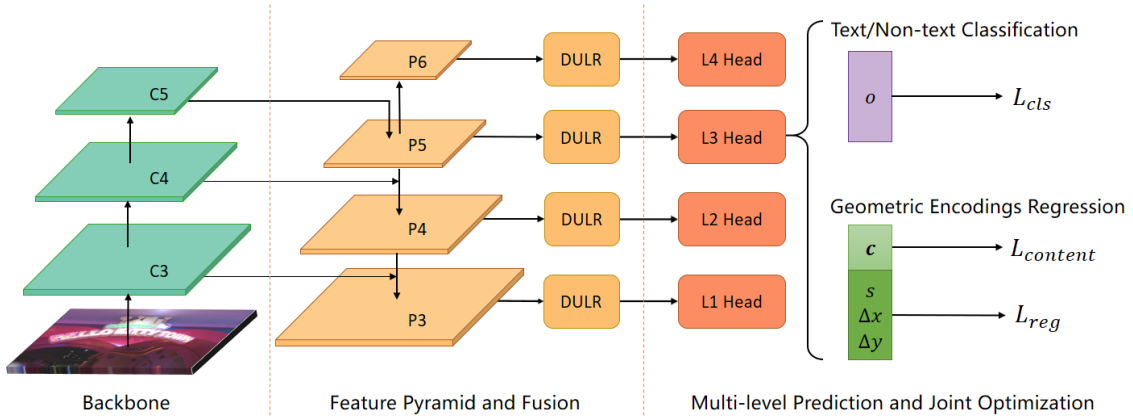


**Figure 4: The architecture of TextRay.** The TextRay consists of three parts: feature extraction with a backbone network shown on the left; feature pyramid generation and global feature fusion in the middle; and two branch multi-task learning shown on the right where text/non-text classification and geometric encodings regression are jointly optimized on multi-level heads.

training strategy for scene texts which specializes in dealing with the long structures of text instances.

At training, our anchor-free detector uses points within ground-truth instances on the feature maps to conduct regression tasks. Points near the ends of a long text instance could be far from the text center, making it hard to accurately sense the comprehensive geometric information. To guarantee the recall rate and suppress false positives from those long-shot points, we adopt a central-weighted training strategy.

Specifically, points on the feature maps are classified into three categories: positive points that locate in a ground-truth polygon, negative points that are outside of all ground-truth polygons and ignored points that belong to hard instances. Given a ground-truth text instance whose  $\mathbf{ge} = [c, s, x, y]$ , the central weight of the  $i$ -th inside positive point  $(x_i, y_i)$  is determined according to its distance from the text center:

$$w_i = 1 - \frac{\sqrt{(x_i - x)^2 + (y_i - y)^2}}{s}. \quad (5)$$

The central weights are applied twice during the training process. Firstly, the positive point is given a probability  $p_i$  of being sampled into a mini-batch according to its central weights:

$$p_i = \frac{w_i}{\sum_{j=0}^M w_j}, \quad (6)$$

where  $M$  is the number of all positive points in a training image. Secondly, once a mini-batch is sampled, the training weights of each point in it (the original weight is 1) will be re-distributed on the basis of central weights and keep the sum of weights within a mini-batch unchanged:

$$q_i = \frac{w_i M'}{\sum_{j=0}^{M'} w_j}, \quad (7)$$

where  $M'$  is the number of positive points within the current mini-batch and  $q_i$  is the training weight of the current point.  $q_i$  is applied on all positive points in all training tasks. Note that for negative points,  $q_i = 1$  in the classification task.

Consequently, the nearer a positive point is to the text center, the more frequently and significantly it would be involved in the

training tasks. Different from centerness proposed in FCOS, we re-weight different points in the training stage and no affiliated scores need to be predicted during testing.

**Loss function.** The TextRay adopts two-branch multi-task joint optimization. For the text/non-text classification branch, the label  $o^*$  for positive/negative points are set to 1/0 respectively. For the geometric encodings regression branch, only positive points are involved. The overall loss function of the TextRay is as follows:

$$L = \frac{1}{N_{cls}} \sum_i^{N_{cls}} q_i L_{cls}(o_i, o_i^*) + \frac{1}{N_{reg}} \sum_j^{N_{reg}} q_j L_{content}(c_j, c_j^*) + \frac{1}{N_{reg}} \sum_j^{N_{reg}} q_j L_{reg}(t_j, t_j^*). \quad (8)$$

where  $L_{cls}$  is the classification loss,  $L_{content}$  and  $L_{reg}$  are losses for geometric encodings.  $t_j = [s_j, \Delta x_j, \Delta y_j]$  represents the scale and center point offset targets of positive point  $j$ .  $c_j$  is the predicted shape vector of the  $j$ -th positive point.  $o_i$  is the predicted probability of the  $i$ -th point being text region.  $o_i^*$ ,  $c_j^*$  and  $t_j^*$  are the ground-truth values.

Similar to RPN [25],  $L_{cls}$  is a two-class softmax loss for classification task.  $L_{content}$  is the content loss introduced in Section 3.2, and  $L_{reg}$  is the smooth- $L_1$  loss. These three terms are normalized by  $N_{cls}$  and  $N_{reg}$ , where  $N_{reg}$  is the number of positive points and  $N_{cls}$  is the number of positive and negative points combined.

## 4 EXPERIMENTS

### 4.1 Datasets

We evaluate the TextRay on three standard arbitrary-shaped scene text detection benchmarks: SCUT-CTW1500 [16], TotalText [4] and ICDAR-ArT [5].

**SCUT-CTW1500.** SCUT-CTW1500 [16] is a challenging dataset that contains multi-oriented, curved and irregular-shaped text. It consists of 1000 training images and 500 test images. SCUT-CTW1500 dataset provides text line-level annotations in the form of 14 vertices.

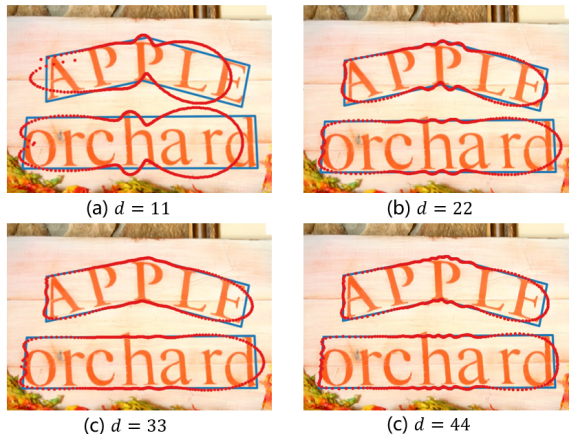


**Figure 5: Visualization of reconstructed contours (red) from 11, 22, 33 and 44-degree Chebyshev polynomials fitting and ground-truth polygons (blue). As shown in the figures, the reconstruction error decreases with higher fitting degree.**

**TotalText.** TotalText [4] is another curved text benchmark which consist of 1255 training images and 300 test images. This dataset includes horizontal, multi-oriented, and curved texts. Different from SCUT-CTW1500, the texts in TotalText are labeled at word level with adaptive number of vertices.

**ICDAR-ArT.** ICDAR-ArT [5] is a large-scale multi-lingual arbitrary-shaped text detection benchmark. It consists of 5603 training images and 4563 test images. Note that the whole datasets of SCUT-CTW1500 and TotalText are included in the training set of ICDAR-ArT with changes in RGB and annotation style. The text regions are labeled with polygons annotated by adaptive number of vertices.

We adopt the same standard evaluation metric as the ICDAR challenges for all experiments.

## 4.2 Implementation Details

Our TextRay is implemented on PyTorch [24] and MMDetection [3]. We use ResNet50 [11] pre-trained on ImageNet [26] as our backbone and adopt the FPN [13] neck for multi-level feature maps. For the training on SCUT-CTW1500 and TotalText, we employ  $\{P_3, P_4, P_5, P_6\}$  of the FPN whose resolutions scale from  $8 \times 8$  to  $64 \times 64$  down-sampling of the input image. And the according relative size ranges of multi-level prediction are  $[0, 0.3]$ ,  $[0.2, 0.55]$ ,  $[0.45, 0.8]$  and  $[0.7, \infty]$ . For the training on ICDAR-ArT, we add an extra  $P_7$  whose resolution is  $128 \times 128$  down-sampling of the input image, for the scales of samples in ICDAR-ArT change more drastically. And the multi-level ranges are set as  $[0, 0.25]$ ,  $[0.15, 0.45]$ ,  $[0.35, 0.65]$ ,  $[0.55, 0.85]$  and  $[0.75, \infty]$ .

The TextRay is optimized end-to-end by using stochastic gradient descent (SGD) with a momentum of 0.9 and weight decay of 0.0001. We adopt the ‘‘cosine’’ policy to adjust the learning rate which starts at 0.08. An online data augmentation strategy is adopted: first we conduct random color jitter, then we randomly crop a square region on each image, and resize the cropped image to  $960 \times 960$ . The consequent rescale factors with respect to the origin resolution are limited within ranges  $[0.5, 4]$ ,  $[0.5, 5]$  and  $[0.5, 6]$  for ICDAR-ArT, SCUT-CTW1500 and TotalText, respectively. Regions cropped out of the image boundary will be padded with zeros. We train the

**Table 1: Results on SCUT-CTW1500.**

Method	Precision	Recall	F-measure
TextSnake [20]	67.90	<b>85.30</b>	75.60
LOMO [39]	<b>89.20</b>	69.60	78.40
CSE [18]	81.10	76.00	78.40
PSENet-4s [30]	82.09	77.84	79.90
Wang <i>et al.</i> [32]	80.10	80.20	80.10
SAST [29]	85.31	77.05	80.97
TextField [36]	83.00	79.80	81.40
<b>TextRay</b>	82.80	80.35	<b>81.56</b>

**Table 2: Results on TotalText.**

Method	Precision	Recall	F-measure
TextSnake [20]	82.70	74.50	78.40
Wang <i>et al.</i> [32]	80.90	76.20	78.50
PSENet-4s [30]	85.54	75.23	79.61
SAST [29]	83.77	76.86	80.17
CSE [18]	81.40	79.10	80.20
TextDragon [8]	<b>85.60</b>	75.70	80.30
TextField [36]	81.20	<b>79.90</b>	<b>80.60</b>
<b>TextRay</b>	83.49	77.88	80.59

models for 300 epochs on ICDAR-ArT and 500 epochs on SCUT-CTW1500 and TotalText with batch size 24 on 4 Titan X (Pascal). During training, the negative/positive ratio of sampling ranges from 1 to 3. In the test stage, for each predicted geometric encoding we reconstruct 360 points on the contour and uniformly sample 36 points according to the perimeter as the final polygon detection.

## 4.3 Evaluation on SCUT-CTW1500

We evaluate our TextRay on SCUT-CTW1500 which contains challenging rotated, curve and long line-level instances. The fitting degree of Chebyshev polynomials is set to  $K = 44$  in this case. For the lack of arbitrary-shaped text dataset, we conduct pre-training on a selected subset from ICDAR-ArT by excluding the test set of SCUT-CTW1500. We pre-train on the selected dataset for 300 epochs and fine-tune on SCUT-CTW1500 for 500 epochs. The initial learning rate of fine-tuning stage is set to 0.01. To deal with hard negatives, we regard points on feature maps with central weights smaller than 0.1 as negative samples, those from 0.1 to 0.4 as ignored samples and those with central weights over 0.4 as positive samples. During testing, we resize the test images to the maximum size of  $800 \times 640$ , keeping the aspect ratios unchanged. We take detections whose predicted scores are over 0.95 as final results.

Quantitative results are shown in Table 1. As a light-weighted one-stage regression-based detector, the TextRay outperforms many segmentation-based and two-stage detectors according to the statistics and achieve competitive results on SCUT-CTW1500. The qualitative results of SCUT-CTW1500 dataset is shown in the first line of Figure 6. As we can see, the TextRay is able to accurately detect rotated, curve, irregular and long text lines.

## 4.4 Evaluation on TotalText

We also evaluate our TextRay on TotalText which contains word-level instances. The fitting degree of Chebyshev polynomials is set to  $K = 33$  in this case. Similar to SCUT-CTW1500, we exclude the test set of TotalText from ICDAR-ArT to conduct pre-training. The training settings are the same with SCUT-CTW1500. For the



Figure 6: Qualitative results on SCUT-CTW1500 (first line) and TotalText (second line). The 36-point detections are visualized as green polygons.

Table 3: Results of different modeling methods and fitting degrees on ICDAR-ArT, SCUT-CTW1500 and TotalText.

Method	ICDAR-ArT			SCUT-CTW1500			TotalText		
	Precision	Recall	F-measure	Precision	Recall	F-measure	Precision	Recall	F-measure
TextRay_Cartesian	71.77	51.71	60.11	78.70	75.52	77.08	78.39	71.11	74.57
TextRay_360r	<b>78.24</b>	57.11	66.03	79.26	77.09	78.16	79.58	75.67	77.57
TextRay_cheby_11d	71.69	53.90	61.54	74.21	68.84	71.42	80.64	72.42	76.31
TextRay_cheby_22d	75.30	58.22	65.67	78.95	76.27	77.59	79.95	75.26	77.53
TextRay_cheby_33d	74.80	58.60	65.74	<b>80.22</b>	77.48	78.83	<b>81.05</b>	<b>76.66</b>	<b>78.79</b>
TextRay_cheby_44d	75.97	58.60	<b>66.17</b>	79.69	78.16	78.92	80.96	75.62	78.20
TextRay_cheby_55d	74.94	<b>58.80</b>	65.90	79.79	77.57	78.66	80.11	74.72	77.32
TextRay_cheby_66d	75.82	58.60	66.11	80.19	<b>78.36</b>	<b>79.26</b>	80.35	75.30	77.74

instances are at word level, to maintain a higher recall rate, we regard points with central weights equal to 0 as negative samples, those from 0 to 0.1 as ignored samples and those with central weights over 0.1 as positive samples. In the test stage, we resize the test images to the maximum size of  $960 \times 960$  while preserving the aspect ratios. Detections with classification scores over 0.995 are taken as final results.

The quantitative results are shown in Table 2. According to the statistics, the TextRay surpasses many state-of-the-art methods and achieves competitive results on word-level TotalText dataset. The second line in Figure 6 shows some qualitative results on TotalText. As demonstrated, the TextRay successfully detects arbitrary-shaped text instances at word-level.

#### 4.5 Ablation Study

We conduct a series of ablation studies on ICDAR-ArT, SCUT-CTW1500 and TotalText to demonstrate the effectiveness of our global geometric modeling method and the TextRay framework. All experiments in this section are conducted *without pre-training*. When testing on ICDAR-ArT, the test images are re-scaled to  $[1280, 960]$  with aspect ratio unchanged, and the negative and positive thresholds of central weights are set to 0.1 and 0.2. A predicted polygon is taken as a detection if its classification score is over 0.99.

**Influence of fitting degrees.** The space mapping of contours from shape space to parameter space through Chebyshev polynomials curve fitting is a process with error. As shown in Figure 5, the reconstruction error decreases with higher fitting degrees and thus improve the performance of our TextRay. However, while the fitting degree increases, the error decrease slows down and the learning difficulty increases. To study the trade-off between reconstruction error and training difficulty, we conduct a set of comparisons on fitting degree. The third to the last lines in Table 3 shows that as the fitting degree going up, the performance reaches a bottleneck. More specifically, for long line-level instances (SCUT-CTW1500), the optimal fitting degree is higher than word-level instances (TotalText). The reason is that the larger the aspect ratio is, the larger deviation the curve would preserve, and thus more parameters are needed during curve fitting. As a trade-off, we choose 33-degree Chebyshev polynomials for word-level TotalText and 44-degree for line-level SCUT-CTW1500 in our experiments.

**Comparison with other global modelings.** To demonstrate the effectiveness of our global geometric modeling method, we conduct two comparisons. The first one is the given global modeling for arbitrary-shaped texts in the benchmarks, that are, polygons denoted by adaptive number (ICDAR-ArT and TotalText) or fixed number (SCUT-CTW1500) of points in Cartesian coordinates. To



**Table 4: Evaluation of content loss and central-weighted training strategy on SCUT-CTW1500.**

ContentLoss	CentralWeight	Precision	Recall	F-measure
		75.71	71.12	73.34
✓		78.97	76.01	77.46
	✓	77.45	75.10	76.25
✓	✓	<b>79.69</b>	<b>78.16</b>	<b>78.92</b>

embed the non-unified representation into our framework, we extend all the ground-truths in ICDAR-ArT and TotalText datasets into 12 points by interpolation. On SCUT-CTW1500 dataset we directly use its 14-point polygon annotations. The regression targets are the offsets from the current location on the feature map to the 12 or 14 points under Cartesian system. This experiment is denoted by *TextRay\_Cartesian*. The second comparison is to directly use the sampled 360 radiuses as the global representation of instances. The regression targets for this experiment are 360 normalized radiuses, normalization factor  $s$ , and center point offset  $(\Delta x, \Delta y)$ . We name this experiment *TextRay\_360r*. In these comparison experiments, independent points or radiuses are directly regressed in the TextRay framework with smooth-L1 loss under the same training settings. Table 3 shows the experimental results of different modeling methods. As we can see, the intuitive global modeling method *TextRay\_Cartesian* does not perform well in arbitrary-shaped text detection. And the *TextRay\_360r* performs better against our geometric modeling methods with low fitting degrees but is surpassed by higher fitting degrees. The comprehensive comparisons demonstrate the superiority of our modeling method. Figure 7 shows some qualitative results of *TextRay\_cheby\_44d* on ICDAR-ArT dataset.

**Effectiveness of content loss and central-weighted training.** To demonstrate the effectiveness of our proposed content loss and central-weighted training strategy, we carry out comparison experiments on SCUT-CTW1500 on the basis of *TextRay\_cheby\_44d*. Except for the utilization of these two techniques, other experimental settings are all the same. According to the quantitative results in Table 4, the content loss and central-weighted training strategy independently improve the comprehensive performance (i.e., F-measure) by 4.12% and 2.91%, respectively. And when simultaneously employed (i.e., the proposed TextRay), the performance is improved by a large margin of 5.58%.

#### 4.6 Limitation

In this subsection we discuss the limitation of our global geometric modeling method. Though our modeling method achieves good performances on the benchmarks, there are still some intrinsic flaws that cannot be perfectly solved. As illustrated in the left column of Figure 8, for severely non-convex contours, the reconstruction error is already beyond acceptable in the geometric encoding procedure. And thus it is impossible to successfully recover the contours under acceptable error with these geometric encodings in the decoding process. This is because during radiuses sampling, the rays emitted from text center will frequently intersect the contour for more than once. And each time we choose one of the intersections (i.e., the farthest one in this work), we lose a part of the contour information. The missing of information accumulates in severely non-convex contours and makes successful reconstruction impossible. The right column of Figure 8 shows these failed detections of our TextRay.



**Figure 7: Qualitative results on ICDAR-ArT. The 36-point detections are visualized as green polygons.**



**Figure 8: Demonstration of the limitation of our global geometric modeling method. The left column shows the ground-truth polygons (lime) and the reconstructed contours (red) from the ground-truth geometric encodings. The right column shows the detections (green).**

Though severely non-convex instances are of a very small proportion in current benchmarks, solving this limitation in our global modeling method is an important research point of our future work.

## 5 CONCLUSION

In this paper, we propose an arbitrary-shaped scene text detection method, namely TextRay, which conducts contour-based geometric modeling and geometric parameter learning within a single-shot anchor-free framework. We model arbitrary shapes under polar system and represent contours with geometric encodings through bidirectional space mapping between shape space and parameter space. The geometric encodings are effectively learned with the differentiable mapping scheme and central-weighted training strategy. TextRay is able to accurately detect arbitrary-shaped texts and output simple polygon detections at one pass.<sup>1</sup>

<sup>1</sup> **Acknowledgements.** This work is supported by key scientific technological innovation research project by Ministry of Education, Zhejiang Provincial Natural Science Foundation of China under Grant LR19F020004, Baidu AI Frontier Technology Joint Research Program, and Zhejiang University K.P.Chao’s High Technology Development Foundation.



## REFERENCES

- [1] Youngmin Baek, Bado Lee, Dongyoon Han, Sangdoon Yun, and Hwalsuk Lee. 2019. Character Region Awareness for Text Detection. In *IEEE Conference on Computer Vision and Pattern Recognition, CVPR*. IEEE Computer Society, 9365–9374.
- [2] Navaneeth Bodla, Bharat Singh, Rama Chellappa, and Larry S. Davis. 2017. Soft-NMS - Improving Object Detection with One Line of Code. In *IEEE International Conference on Computer Vision, ICCV*. IEEE Computer Society, 5562–5570.
- [3] Kai Chen, Jiaqi Wang, Jiangmiao Pang, Yuhang Cao, Yu Xiong, Xiaoxiao Li, Shuyang Sun, Wansen Feng, Ziwei Liu, Jiarui Xu, Zheng Zhang, Dazhi Cheng, Chenchen Zhu, Tianheng Cheng, Qijie Zhao, Buyu Li, Xin Lu, Rui Zhu, Yue Wu, Jifeng Dai, Jingdong Wang, Jianping Shi, Wanli Ouyang, Chen Change Loy, and Dahua Lin. 2019. MMDetection: Open MMLab Detection Toolbox and Benchmark. *CoRR* abs/1906.07155 (2019).
- [4] Chee Kheng Chng and Chee Seng Chan. 2017. Total-Text: A Comprehensive Dataset for Scene Text Detection and Recognition. In *14th IAPR International Conference on Document Analysis and Recognition, ICDAR*. IEEE Computer Society, 935–942.
- [5] Chee Kheng Chng, Errui Ding, Jingtuo Liu, Dimosthenis Karatzas, Chee Seng Chan, Lianwen Jin, Yuliang Liu, Yipeng Sun, Chun Chet Ng, Canjie Luo, Zihan Ni, ChuanMing Fang, Shuaitao Zhang, and Junyu Han. 2019. ICDAR2019 Robust Reading Challenge on Arbitrary-Shaped Text - RRC-ArT. In *International Conference on Document Analysis and Recognition, ICDAR*. IEEE Computer Society, 1571–1576.
- [6] Dan Deng, Haifeng Liu, Xuelong Li, and Deng Cai. 2018. PixelLink: Detecting Scene Text via Instance Segmentation. In *Proceedings of the Thirty-Second AAAI Conference on Artificial Intelligence*, Sheila A. McIlraith and Kilian Q. Weinberger (Eds.). AAAI Press, 6773–6780.
- [7] Jiaqi Duan, Youjiang Xu, Zhanghui Kuang, Xiaoyu Yue, Hongbin Sun, Yue Guan, and Wayne Zhang. 2019. Geometry Normalization Networks for Accurate Scene Text Detection. In *IEEE International Conference on Computer Vision, ICCV*. IEEE Computer Society, 9136–9145.
- [8] Wei Feng, Wenhao He, Fei Yin, Xu-Yao Zhang, and Cheng-Lin Liu. 2019. TextDragon: An End-to-End Framework for Arbitrary Shaped Text Spotting. In *IEEE International Conference on Computer Vision, ICCV*. IEEE Computer Society, 9075–9084.
- [9] Ross B. Girshick. 2015. Fast R-CNN. In *IEEE International Conference on Computer Vision, ICCV*. IEEE Computer Society, 1440–1448.
- [10] Kaiming He, Georgia Gkioxari, Piotr Dollár, and Ross B. Girshick. 2017. Mask R-CNN. In *IEEE International Conference on Computer Vision, ICCV*. IEEE Computer Society, 2980–2988.
- [11] Kaiming He, Xiangyu Zhang, Shaoqing Ren, and Jian Sun. 2016. Deep Residual Learning for Image Recognition. In *IEEE Conference on Computer Vision and Pattern Recognition, CVPR*. IEEE Computer Society, 770–778.
- [12] Minghui Liao, Zhen Zhu, Baoguang Shi, Gui-Song Xia, and Xiang Bai. 2018. Rotation-Sensitive Regression for Oriented Scene Text Detection. In *IEEE Conference on Computer Vision and Pattern Recognition, CVPR*. IEEE Computer Society, 5909–5918.
- [13] Tsung-Yi Lin, Piotr Dollár, Ross B. Girshick, Kaiming He, Bharath Hariharan, and Serge J. Belongie. 2017. Feature Pyramid Networks for Object Detection. In *IEEE Conference on Computer Vision and Pattern Recognition, CVPR*. IEEE Computer Society, 936–944.
- [14] Wei Liu, Dragomir Anguelov, Dumitru Erhan, Christian Szegedy, Scott E. Reed, Cheng-Yang Fu, and Alexander C. Berg. 2016. SSD: Single Shot MultiBox Detector. In *Computer Vision - ECCV 2016 - 14th European Conference, Proceedings, Part I (Lecture Notes in Computer Science)*, Vol. 9905. Springer, 21–37.
- [15] Yuliang Liu, Hao Chen, Chunhua Shen, Tong He, Lianwen Jin, and Liangwei Wang. 2020. ABCNet: Real-time Scene Text Spotting with Adaptive Bezier-Curve Network. *CoRR* abs/2002.10200 (2020).
- [16] Yuliang Liu, Lianwen Jin, Shuaitao Zhang, Canjie Luo, and Sheng Zhang. 2019. Curved scene text detection via transverse and longitudinal sequence connection. *Pattern Recognit.* 90 (2019), 337–345.
- [17] Zichuan Liu, Guosheng Lin, Sheng Yang, Jiashi Feng, Weisi Lin, and Wang Ling Goh. 2018. Learning Markov Clustering Networks for Scene Text Detection. In *IEEE Conference on Computer Vision and Pattern Recognition, CVPR*. IEEE Computer Society, 6936–6944.
- [18] Zichuan Liu, Guosheng Lin, Sheng Yang, Fayao Liu, Weisi Lin, and Wang Ling Goh. 2019. Towards Robust Curve Text Detection With Conditional Spatial Expansion. In *IEEE Conference on Computer Vision and Pattern Recognition, CVPR*. IEEE Computer Society, 7269–7278.
- [19] Jonathan Long, Evan Shelhamer, and Trevor Darrell. 2015. Fully convolutional networks for semantic segmentation. In *IEEE Conference on Computer Vision and Pattern Recognition, CVPR*. IEEE Computer Society, 3431–3440.
- [20] Shangbang Long, Jiaqi Ruan, Wenjie Zhang, Xin He, Wenhao Wu, and Cong Yao. 2018. TextSnake: A Flexible Representation for Detecting Text of Arbitrary Shapes. In *Computer Vision - ECCV 2018 - 15th European Conference, Proceedings, Part II*, Vol. 11206. Springer, 19–35.
- [21] Pengyuan Lyu, Minghui Liao, Cong Yao, Wenhao Wu, and Xiang Bai. 2018. Mask TextSpotter: An End-to-End Trainable Neural Network for Spotting Text with Arbitrary Shapes. In *Computer Vision - ECCV 2018 - 15th European Conference, Proceedings, Part XIV*, Vittorio Ferrari, Martial Hebert, Cristian Sminchisescu, and Yair Weiss (Eds.), Vol. 11218. Springer, 71–88.
- [22] Pengyuan Lyu, Cong Yao, Wenhao Wu, Shuicheng Yan, and Xiang Bai. 2018. Multi-Oriented Scene Text Detection via Corner Localization and Region Segmentation. In *IEEE Conference on Computer Vision and Pattern Recognition, CVPR*. IEEE Computer Society, 7553–7563.
- [23] Xingang Pan, Jianping Shi, Ping Luo, Xiaogang Wang, and Xiaoou Tang. 2018. Spatial as Deep: Spatial CNN for Traffic Scene Understanding. In *Proceedings of the Thirty-Second AAAI Conference on Artificial Intelligence*, Sheila A. McIlraith and Kilian Q. Weinberger (Eds.). AAAI Press, 7276–7283.
- [24] Adam Paszke, Sam Gross, Francisco Massa, Adam Lerer, James Bradbury, Gregory Chanan, Trevor Killeen, Zeming Lin, Natalia Gimelshein, Luca Antiga, Alban Desmaison, Andreas Köpf, Edward Yang, Zachary DeVito, Martin Raison, Alykhan Tejani, Sasank Chilamkurthy, Benoit Steiner, Lu Fang, Junjie Bai, and Soumith Chintala. 2019. PyTorch: An Imperative Style, High-Performance Deep Learning Library. In *Advances in Neural Information Processing Systems*. 8024–8035.
- [25] Shaoqing Ren, Kaiming He, Ross B. Girshick, and Jian Sun. 2015. Faster R-CNN: Towards Real-Time Object Detection with Region Proposal Networks. In *Advances in Neural Information Processing Systems 28: Annual Conference on Neural Information Processing Systems, NIPS*. 91–99.
- [26] Olga Russakovsky, Jia Deng, Hao Su, Jonathan Krause, Sanjeev Satheesh, Sean Ma, Zhiheng Huang, Andrej Karpathy, Aditya Khosla, Michael S. Bernstein, Alexander C. Berg, and Fei-Fei Li. 2015. ImageNet Large Scale Visual Recognition Challenge. *Int. J. Comput. Vis.* 115, 3 (2015), 211–252.
- [27] Zhi Tian, Chunhua Shen, Hao Chen, and Tong He. 2019. FCOS: Fully Convolutional One-Stage Object Detection. In *IEEE International Conference on Computer Vision, ICCV*. IEEE Computer Society, 9626–9635.
- [28] Fangfang Wang, Liming Zhao, Xi Li, Xinchao Wang, and Dacheng Tao. 2018. Geometry-Aware Scene Text Detection With Instance Transformation Network. In *IEEE Conference on Computer Vision and Pattern Recognition, CVPR*. IEEE Computer Society, 1381–1389.
- [29] Pengfei Wang, Chengquan Zhang, Fei Qi, Zuming Huang, Mengyi En, Junyu Han, Jingtuo Liu, Errui Ding, and Guangming Shi. 2019. A Single-Shot Arbitrarily-Shaped Text Detector based on Context Attended Multi-Task Learning. In *Proceedings of the 27th ACM International Conference on Multimedia, MM*. ACM, 1277–1285.
- [30] Wenhao Wang, Enze Xie, Xiang Li, Wenbo Hou, Tong Lu, Gang Yu, and Shuai Shao. 2019. Shape Robust Text Detection With Progressive Scale Expansion Network. In *IEEE Conference on Computer Vision and Pattern Recognition, CVPR*. IEEE Computer Society, 9336–9345.
- [31] Wenhao Wang, Enze Xie, Xiaohe Song, Yuhang Zang, Wenjie Wang, Tong Lu, Gang Yu, and Chunhua Shen. 2019. Efficient and Accurate Arbitrarily-Shaped Text Detection With Pixel Aggregation Network. In *IEEE International Conference on Computer Vision, ICCV*. IEEE Computer Society, 8439–8448.
- [32] Xiaobing Wang, Yingying Jiang, Zhenbo Luo, Cheng-Lin Liu, Hyunsoo Choi, and Sungjin Kim. 2019. Arbitrary Shape Scene Text Detection With Adaptive Text Region Representation. In *IEEE Conference on Computer Vision and Pattern Recognition, CVPR*. IEEE Computer Society, 6449–6458.
- [33] Yuxin Wang, Hongtao Xie, Zhengjun Zha, Mengting Xing, Zilong Fu, and Yongdong Zhang. 2020. ContourNet: Taking a Further Step toward Accurate Arbitrarily-shaped Scene Text Detection. *CoRR* abs/2004.04940 (2020).
- [34] Enze Xie, Peize Sun, Xiaoge Song, Wenhao Wang, Xuebo Liu, Ding Liang, Chunhua Shen, and Ping Luo. 2019. PolarMask: Single Shot Instance Segmentation with Polar Representation. *CoRR* abs/1909.13226 (2019).
- [35] Wenqiang Xu, Haiyang Wang, Fubo Qi, and Cewu Lu. 2019. Explicit Shape Encoding for Real-Time Instance Segmentation. In *IEEE International Conference on Computer Vision, ICCV*. IEEE Computer Society, 5167–5176.
- [36] Yongchao Xu, Yukang Wang, Wei Zhou, Yongpan Wang, Zhibo Yang, and Xiang Bai. 2019. TextField: Learning a Deep Direction Field for Irregular Scene Text Detection. *IEEE Trans. Image Processing* 28, 11 (2019), 5566–5579.
- [37] Ze Yang, Yinghao Xu, Han Xue, Zheng Zhang, Raquel Urtasun, Liwei Wang, Stephen Lin, and Han Hu. 2019. Dense RepPoints: Representing Visual Objects with Dense Point Sets. *CoRR* abs/1912.11473 (2019).
- [38] Cong Yao, Xiang Bai, Nong Sang, Xinyu Zhou, Shuchang Zhou, and Zhimin Cao. 2016. Scene Text Detection via Holistic, Multi-Channel Prediction. *CoRR* abs/1606.09002 (2016).
- [39] Chengquan Zhang, Borong Liang, Zuming Huang, Mengyi En, Junyu Han, Errui Ding, and Xinghao Ding. 2019. Look More Than Once: An Accurate Detector for Text of Arbitrary Shapes. In *IEEE Conference on Computer Vision and Pattern Recognition, CVPR*. IEEE Computer Society, 10552–10561.
- [40] Zheng Zhang, Chengquan Zhang, Wei Shen, Cong Yao, Wenyu Liu, and Xiang Bai. 2016. Multi-oriented Text Detection with Fully Convolutional Networks. In *IEEE Conference on Computer Vision and Pattern Recognition, CVPR*. IEEE Computer Society, 4159–4167.